

# Visible Light Driven Water Splitting in a Molecular Device with Unprecedentedly High Photocurrent Density

Yan Gao,<sup>\*,†</sup> Xin Ding,<sup>†</sup> Jianhui Liu,<sup>†</sup> Lei Wang,<sup>‡</sup> Zhongkai Lu,<sup>†</sup> Lin Li,<sup>‡</sup> and Licheng Sun<sup>\*,†,‡</sup>

<sup>†</sup>State Key Laboratory of Fine Chemicals, Dalian University of Technology (DUT), DUT-KTH Joint Education and Research Center on Molecular Devices, Dalian 116024, China

<sup>‡</sup>Department of Chemistry, School of Chemical Science and Engineering, KTH Royal Institute of Technology, 100 44 Stockholm, Sweden

**S** Supporting Information

**ABSTRACT:** A molecular water oxidation catalyst (2) has been synthesized and immobilized together with a molecular photosensitizer (1) on nanostructured TiO<sub>2</sub> particles on FTO conducting glass, forming a photoactive anode (TiO<sub>2</sub>(1+2)). By using the TiO<sub>2</sub>(1+2) as working electrode in a three-electrode photoelectrochemical cell (PEC), visible light driven water splitting has been successfully demonstrated in a phosphate buffer solution (pH 6.8), with oxygen and hydrogen bubbles evolved respectively from the working electrode and counter electrode. By applying 0.2 V external bias vs NHE, a high photocurrent density of more than 1.7 mA·cm<sup>-2</sup> has been achieved. This value is higher than any PEC devices with molecular components reported in literature.

To meet the global demand for sustainable energy systems, there is increasing focus on converting solar energy into chemical energy, such as hydrogen via visible light driven water splitting.<sup>1</sup> In practical design, several photoelectrochemical cells (PECs) have been reported very recently for light driven water splitting.<sup>2–16</sup> Most of these PECs were assembled with inorganic materials as anodes,<sup>5–10,15</sup> and only very few PECs were assembled using molecular components.<sup>11–14</sup> These reported molecular PECs displayed relatively low photocurrent densities by even applying high external bias.<sup>11–13</sup> Therefore, a key challenge in this field is to develop a PEC which can achieve light driven water splitting with a high photocurrent density by applying a small external bias or even no bias. Recently, a literature reported a PEC with a photoanode composed of 3P–Ru dye as photosensitizer, IrO<sub>x</sub> linked by 2-carboxyethylphosphonic acid (CEPA) as catalyst. A photocurrent density of 150 μA/cm<sup>2</sup> after 10 s light illumination with a low external bias of 0.2 V (vs NHE) has been observed.<sup>14</sup> Here, we report a new PEC device using molecular catalyst giving a much higher photocurrent density of more than 1.7 mA·cm<sup>-2</sup>. This result moves a big step forward toward more practical devices for solar energy conversion into chemical energy.

Encouraged by the successful development of highly efficient molecular catalysts for water oxidation in our group,<sup>16–20</sup> a PEC device with one molecular ruthenium catalyst deposited on photoactive TiO<sub>2</sub> electrode coated by a Nafion membrane was assembled.<sup>12</sup> However, the efficiency of this PEC was low,

which might be caused by the strongly acidic Nafion membrane involved, and subsequently increased thermodynamic potential for water oxidation. Therefore, alternative approach without using Nafion as supporting material is needed. We have now successfully demonstrated a new molecular device with co-adsorption of a molecular photosensitizer 1 and a molecular water oxidation catalyst 2 directly on the TiO<sub>2</sub>-sintered FTO glass as a photoactive working electrode (TiO<sub>2</sub>(1+2)), as illustrated in Figure 1.

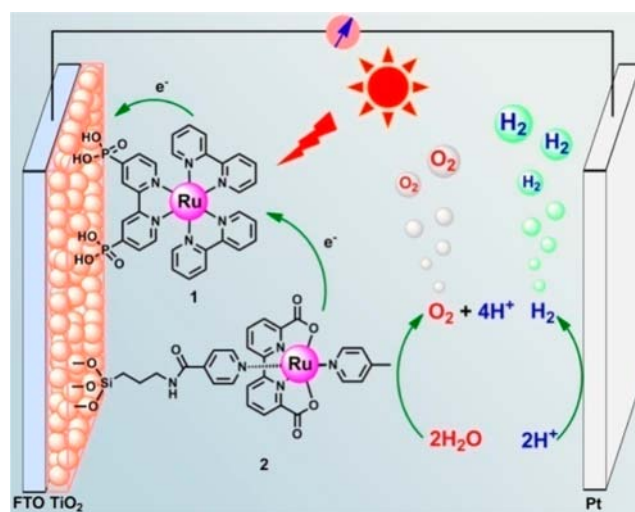


**Figure 1.** Schematic illustration of the molecular device with a photoanode co-adsorbed with photosensitizer [Ru(bpy)<sub>2</sub>(4,4-(PO<sub>3</sub>H<sub>2</sub>)<sub>2</sub>bpy)]Br<sub>2</sub> (1) and a molecular Ru catalyst (2) on nanostructured TiO<sub>2</sub> (TiO<sub>2</sub>(1+2)), and a passive Pt cathode, for visible light driven water splitting in aqueous solution.

Silica–titania-based organic–inorganic hybrid materials (OIHMs) have been widely used in many research fields.<sup>21–23</sup>

It has been shown that triethoxy(methyl) silane group can attach to nano-TiO<sub>2</sub> surface firmly. Here, we have modified our molecular Ru water oxidation catalyst with a silane group, Ru(II)(bda)(4-picoline)L (H<sub>2</sub>bda = bipyridine-dicarboxylic acid; L = N-(3-(triethoxysilyl)propyl)isonicotinamide) (2), and made a photoactive anode using this molecular catalyst 2

Received: January 19, 2013

Published: March 6, 2013

together with a photosensitizer **1** by self-assembly (see the chemical structures of photosensitizer, the catalyst, and the construction of PEC in Figure 1). The flexible carbon chain between the silane anchoring group and the Ru catalyst has been designed by considering a certain mobility of the catalyst on TiO<sub>2</sub> surface to benefit catalysis, which may improve the electron transfer efficiency between photosensitizer and the catalysts, and even facilitate the water oxidation process during its catalytic cycle (for example, radical coupling mechanism for the O–O bond formation requires two Ru catalysts in a close distance).

For preparation of such a device, a TiO<sub>2</sub>-sintered FTO electrode was immersed in a methanol solution containing both molecular photosensitizer **1** and catalyst **2** for 2 h. The electrode was then washed with methanol and water several times and dried in dark at room temperature, forming the working photoanode TiO<sub>2</sub>(1+2). In the same manner, TiO<sub>2</sub>-sintered FTO electrodes adsorbed with only photosensitizer **1** (TiO<sub>2</sub>(1)) or with only catalyst **2** (TiO<sub>2</sub>(2)) have also been prepared as references (see Supporting Information (SI), S2.2).

The cyclic voltammograms (CVs) of the working electrode TiO<sub>2</sub>(1+2) (as shown in Figure 2), and control electrodes

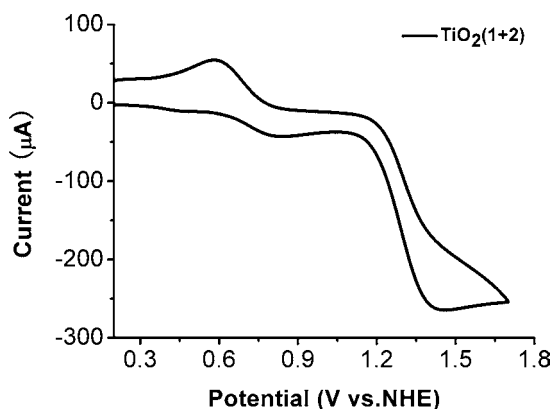


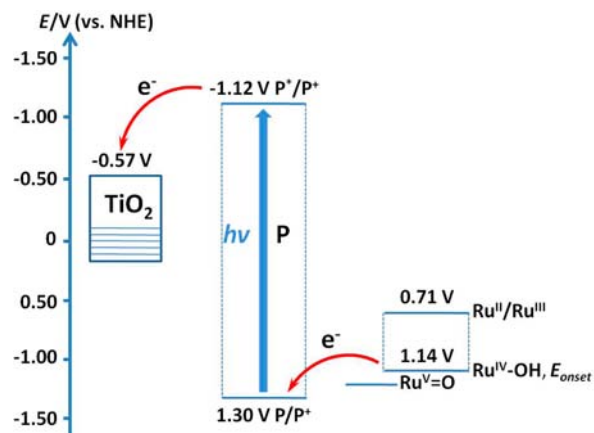
**Figure 2.** Cyclic voltammogram of the working electrode TiO<sub>2</sub>(1+2) in phosphate buffer solution (pH 6.8), Ag/AgCl as reference electrode and Pt wire as counter electrode (potential vs NHE:  $E_{\text{NHE}} = E_{\text{Ag/AgCl}} + 0.20 \text{ V}$ ).

TiO<sub>2</sub>(1) and TiO<sub>2</sub>(2) (as shown in Figure S1) were taken in phosphate buffer solution (pH 6.8). The CV curve in Figure S1a displays a reversible peak at  $E_{1/2} = 1.30 \text{ V}$  (vs NHE) which is assigned to the Ru<sup>II</sup>/Ru<sup>III</sup> redox couple of the photosensitizer **1**. In comparison to this reversible redox peak in Figure S1, the irreversible oxidation peak at  $E_{\text{pa}} = 1.40 \text{ V}$  (vs NHE) in Figure 2 can be assigned to the Ru<sup>II</sup>/Ru<sup>III</sup> of photosensitizer **1**, which is riding on the catalytic wave of catalyst **2** with an onset potential of 1.14 V (vs NHE) for the oxidation of water, while the redox process at  $E_{1/2} = 0.71 \text{ V}$  (vs NHE) in Figure 2 can be assigned to the Ru<sup>II</sup>/Ru<sup>III</sup> redox couple of the catalyst **2** comparing with the CV curve of TiO<sub>2</sub>(2) in Figure S1b. In addition, no catalytic wave could be observed in the reference electrode TiO<sub>2</sub>(1) which without the catalyst **2** absorbed (Figure S1a). Moreover, following the method reported by Meyer et al,<sup>24,25</sup> the surface loading of catalyst **2** in working electrode TiO<sub>2</sub>(1+2) was estimated by the area under the CV wave of the Ru<sup>II</sup>/Ru<sup>III</sup> at  $E_{1/2} = 0.71 \text{ V}$  to be  $8.38 \times 10^{-10} \text{ mol/cm}^2$ . Furthermore, based on the CV of working electrode TiO<sub>2</sub>(1+2) in CH<sub>3</sub>CN (Figure S1c), without the influence of catalytic current of water oxidation, the ratio of photosensitizer **1** and catalyst **2** can be

calculated as about 3:1 by the area of the oxidation peaks of photosensitizer **1** and catalyst **2**.

The energy levels and proposed electron transfer processes in our PEC system were shown in Scheme 1, The energy levels

**Scheme 1.** Energy Levels and Proposed Electron Transfer Processes in Our PEC System (vs NHE)



of photosensitizer **1** and catalyst **2** are electrochemically determined values,  $E(\text{P}^*/\text{P}^+)$  was taken from literature.<sup>13</sup> First, the photosensitizer **1** was excited to reach the excited state  $E(\text{P}^*)$ , which would then transfer electron to nano TiO<sub>2</sub> semiconductor and form an oxidation state  $E(\text{P}^+)$ . Then catalyst **2** transferred an electron to the oxidation state  $E(\text{P}^+)$ , to form Ru<sup>III</sup>, which would combine with water and be oxidized subsequently to form an active intermediate Ru<sup>IV</sup>-OH ( $E_{\text{onset}}$ ). According to the mechanism study in our previous work, Ru<sup>IV</sup>-OH complex can be oxidized continually to form intermediate Ru<sup>V</sup>=O, which undergoes intermolecular O–O radical coupling to release oxygen.<sup>16</sup> However, other mechanisms, such as nucleophilic attack of water, cannot be excluded at this stage.<sup>19</sup>

A three-electrode PEC was built with the photoanode TiO<sub>2</sub>(1+2) as working electrode, Ag/AgCl as reference electrode and Pt wire as cathode for visible light ( $\lambda > 400 \text{ nm}$ )-driven water-splitting (see cell configuration in Figure 1). An external bias of 0.2 V (vs NHE) was applied and the photocurrents in different electrolyte were measured as shown in Figure S2. Inspired by the previous works,<sup>2,3,11,12</sup> 0.1 M Na<sub>2</sub>SO<sub>4</sub> aqueous solution (pH = 6.4) has been used first and a much higher photocurrent density was achieved (Figure S2a, pink line). This exciting result may cause by the high efficient catalytic ability of catalyst on water oxidation with a low over potential.<sup>16,17</sup> Different electrolytes, such as 0.1 M CaCl<sub>2</sub> aqueous solution (pH = 6.7), 0.1 M NaCl aqueous solution (pH = 6.9), potassium acid phthalate buffer solution (pH = 4.0), and phosphate buffer solution (pH = 6.8), have been studied as shown in Figure S2a. All the generated photocurrent densities were very high. Especially, a significant photocurrent density of 1.7 mA/cm<sup>2</sup> in phosphate buffer solution (pH = 6.8) was found. Further studies were performed on the same pH values, the photocurrent densities in phosphate buffer (pH 6.4 or 8.0) were much higher than that in 0.1 M Na<sub>2</sub>SO<sub>4</sub> aqueous (pH 6.4) and borate buffer (pH 8.0), which were shown in Figure S2b,c. The results suggest that phosphate buffer is benefit for enhancement in photocurrent.<sup>10</sup>

Moreover, the pH value effects the photocurrent in phosphate buffer as shown in Figure 3. When the pH value

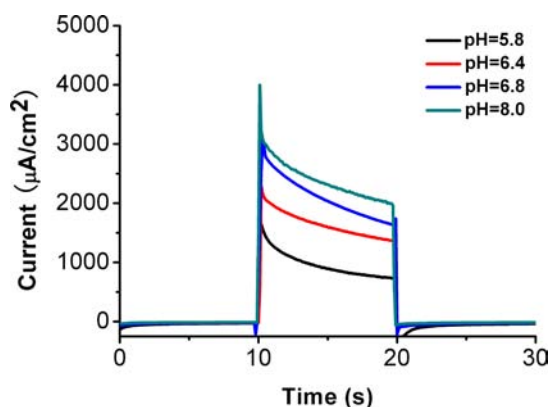


**Figure 3.** Light control photocurrent measurements in a three-electrode cell using  $\text{TiO}_2(1+2)$  ( $0.8 \text{ cm}^2$ ) as working electrode in phosphate buffer solutions, applied external bias:  $0.2 \text{ V}$  (vs NHE); with a white-light source coupled to a  $400 \text{ nm}$  long-pass filter,  $300 \text{ mW/cm}^2$ . For pH 5.8 (black line), pH 6.4 (red line), pH 6.8 (blue line), pH 8.0 (green line).

was controlled at 5.8, an initial photocurrent density of  $1.8 \text{ mA}\cdot\text{cm}^{-2}$  and a final photocurrent density of ca.  $0.80 \text{ mA}\cdot\text{cm}^{-2}$  were found after 10 s light illumination (black line in Figure 3). When using 6.4 pH buffer, the initial and final photocurrent densities were found to be 2.3 and  $1.4 \text{ mA}\cdot\text{cm}^{-2}$ . By increasing the pH to 6.8, the data were found to be 3.1 and  $1.7 \text{ mA}\cdot\text{cm}^{-2}$ , respectively. When the pH value was raised to 8.0, both highest initial photocurrent density of  $4.0 \text{ mA}\cdot\text{cm}^{-2}$  and final photocurrent density of more than  $2.0 \text{ mA/cm}^2$  were obtained. These results indicate that the pH value in phosphate buffer has apparent effect on the photocurrent density of PEC. However, considering that the water splitting in photosystem II normally happens under the neutral condition, we selected the pH 6.8 phosphate buffer for further study.

Photocurrent measurements by applying different external bias were therefore conducted in phosphate buffer solution (pH 6.8). From the CV measurement of the  $\text{TiO}_2(1+2)$  working electrode under light illumination (the black line in Figure S4), we found that the photocurrent density reached the maximum at ca.  $0.2 \text{ V}$  (vs NHE), and no further increase of the photocurrent density at higher potentials. These results are in agreement with the measurements of photocurrent density performed at different bias (see Figure 4). In addition, contrasting CV measurements show that the current densities of working electrodes  $\text{TiO}_2(1)$  and  $\text{TiO}_2(2)$  are not increasing under the light illumination (Figure S4b).

Moreover, after 100 s, of visible light illumination of the working electrode  $\text{TiO}_2(1+2)$  in phosphate buffer solution with  $0.2 \text{ V}$  (vs NHE) external bias, a still very high photocurrent density of ca.  $0.7 \text{ mA}\cdot\text{cm}^{-2}$  (Figure 4, black line) was found. Changing the working electrode from  $\text{TiO}_2(1+2)$  to  $\text{TiO}_2(1)$  or  $\text{TiO}_2(2)$  in corresponding devices (Figure 4, red line and blue line) led to almost neglected photocurrent densities. All these results indicate that both the molecular photosensitizer **1** and the molecular catalyst **2** are necessary to co-exist on the  $\text{TiO}_2$  surface of the working electrode in order to keep the device in function.

The incident photo-current conversion efficiency (IPCE) spectrum of the PEC cell has also been measured using  $\text{TiO}_2(1+2)$  as working electrode. A maximum IPCE value of 14% has been observed at around  $450 \text{ nm}$  (Figure 5, black

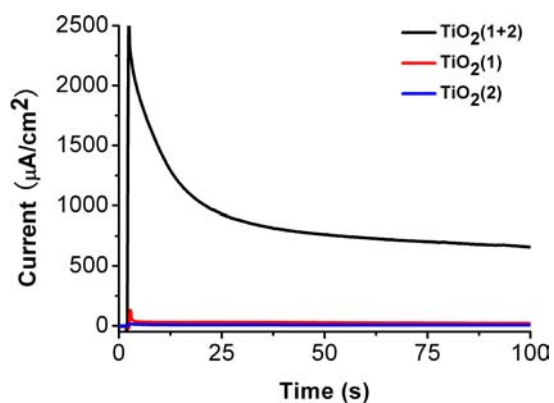


**Figure 4.** Three-electrode light control photocurrent measurements with a  $0.2 \text{ V}$  vs NHE external bias for working electrodes ( $0.8 \text{ cm}^2$ ) in pH = 6.8 phosphate buffer solution upon illumination with a white-light source coupled to a  $400 \text{ nm}$  long-pass filter,  $300 \text{ mW/cm}^2$ , with working electrodes  $\text{TiO}_2(1+2)$  (black line),  $\text{TiO}_2(1)$  (red line) and  $\text{TiO}_2(2)$  (blue line).

line). This result fits well the UV-vis absorption spectrum of the  $\text{TiO}_2(1+2)$  film (Figure S5).

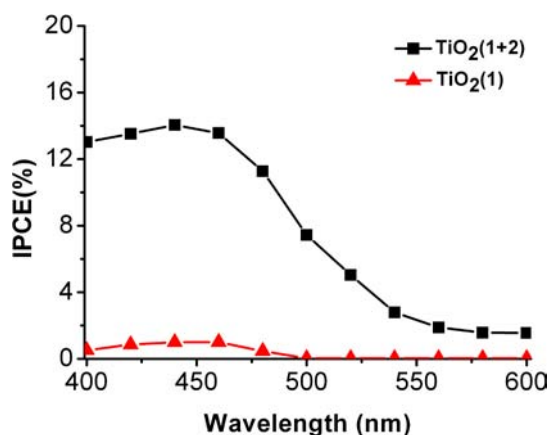


**Figure 5.** IPCE spectra of the PECs in pH 6.8 phosphate buffer solution with a  $0.2 \text{ V}$  vs NHE external bias.

Repeated measurements show that this PEC device works well with applied  $0.2 \text{ V}$  (vs NHE) external bias. A large amount of bubbles have been observed both on the surfaces of working electrode  $\text{TiO}_2(1+2)$  and Pt counter electrode under visible light illumination. The bubbles on working electrode  $\text{TiO}_2(1+2)$  and Pt electrode have been confirmed by GC as oxygen gas and hydrogen gas respectively. Release of both oxygen gas and hydrogen gas during the water splitting process could be seen by naked eyes (see the video in SI). After ca. 500 s of visible light illumination, about  $0.75 \mu\text{mol O}_2$  and  $1.34 \mu\text{mol H}_2$  were detected by GC (Figure S6), and a turnover number (TON) of 498 and an average turnover frequency (TOF) of  $1.0 \text{ s}^{-1}$  for total water splitting based on the molecular catalyst **2** have been calculated. The Faraday efficiency for  $\text{O}_2$  and  $\text{H}_2$  was calculated to 83% and 74%, respectively.

In summary, a PEC device has been successfully assembled using a molecular photosensitizer **1** and a molecular catalyst **2** co-adsorbed on the nanostructured  $\text{TiO}_2$  as the photoanode, and a Pt wire is used as a passive counter electrode. During visible light illumination of this molecular device with applied

0.2 V vs NHE external bias in a three-electrode system, vigorous evolution of both oxygen and hydrogen gases from the respective anode and cathode are observed, showing highly efficient visible light driven water splitting. A record high photocurrent density of more than  $1.7 \text{ mA}\cdot\text{cm}^{-2}$  has been achieved after 10 s light illumination in a phosphate buffer solution (pH 6.8). This value is higher than those so far reported in the literature, making a big step forward toward the final goal of artificial photosynthesis.

## ■ ASSOCIATED CONTENT

### ■ Supporting Information

Full experimental details; control experiments; experimental methods, and Figures S1–S6; water splitting video (avi). This material is available free of charge via the Internet at <http://pubs.acs.org>.

## ■ AUTHOR INFORMATION

### Corresponding Author

[dr.gaoyan@dlut.edu.cn](mailto:dr.gaoyan@dlut.edu.cn); [lichengs@kth.se](mailto:lichengs@kth.se)

### Notes

The authors declare no competing financial interest.

## ■ ACKNOWLEDGMENTS

This work was supported by the National Basic Research Program of China (973 program) (2009CB220009), the National Natural Science Foundation of China (20923006, 21003017, 21120102036, 21106015 and 91233201), the Fundamental Research Funds for the Central Universities, the Swedish Energy Agency and the K & A Wallenberg Foundation.

## ■ REFERENCES

- (1) Grätzel, M. *Nature* **2001**, *414*, 338.
- (2) Youngblood, W. J.; Lee, S.-H. A.; Kobayashi, Y.; Hernandez-Pagan, E. A.; Hoertz, P. G.; Moore, T. A.; Moore, A. L.; Gust, D.; Mallouk, T. E. *J. Am. Chem. Soc.* **2009**, *131*, 926.
- (3) Youngblood, W. J.; Lee, S.-H. A.; Maeda, K.; Mallouk, T. E. *Acc. Chem. Res.* **2009**, *42*, 1966.
- (4) Nann, T.; Ibrahim, S. K.; Woi, P. M.; Xu, S.; Ziegler, J.; Pickett, C. J. *Angew. Chem., Int. Ed.* **2010**, *49*, 1574.
- (5) Kronawitter, C. X.; Vayssieres, L.; Shen, S.; Guo, L.; Wheeler, D. A.; Zhang, J. Z.; Antoun, B. R.; Mao, S. S. *Energy Environ. Sci.* **2011**, *4*, 3889.
- (6) Barroso, M.; Cowan, A. J.; Pendlebury, S. R.; Grätzel, M.; Klug, D. R.; Durrant, J. R. *J. Am. Chem. Soc.* **2011**, *133*, 14868.
- (7) Townsend, T. K.; Sabio, E. M.; Browning, N. D.; Osterloh, F. E. *Energy Environ. Sci.* **2011**, *4*, 4270.
- (8) Maeda, K.; Higashi, M.; Siritanaratkul, B.; Abe, R.; Domen, K. *J. Am. Chem. Soc.* **2011**, *133*, 12334.
- (9) Higashi, M.; Domen, K.; Abe, R. *Energy Environ. Sci.* **2011**, *4*, 4138.
- (10) Higashi, M.; Domen, K.; Abe, R. *J. Am. Chem. Soc.* **2012**, *134*, 6968.
- (11) Moore, G. F.; Blakemore, J. D.; Milot, R. L.; Hull, J. F.; Song, H.; Cai, L.; Schmuttenmaer, C. A.; Crabtree, R. H.; Brudvig, G. W. *Energy Environ. Sci.* **2011**, *4*, 2389.
- (12) Li, L.; Duan, L.; Xu, Y.; Gorlov, M.; Hagfeldt, A.; Sun, L. *Chem. Commun.* **2010**, *46*, 7307.
- (13) Xiang, X.; Fielden, J.; Rodríguez-Córdoba, W.; Huang, Zh.; Zhang, N.; Luo, Zh.; Musaev, D.; Lian, T.; Hill, C. *J. Phys. Chem. C* **2013**, *117*, 916.
- (14) Zhao, Y.; Swierk, J. R.; Megiatto, J. D., Jr; Sherman, B.; Youngblood, W. J.; Qin, D.; Lentz, D. M.; Moore, A. L.; Moore, T. A.; Gust, D.; Mallouk, T. E. *Proc. Natl. Acad. Sci. U.S.A.* **2012**, *109*, 15612.
- (15) Reece, S. Y.; Hamel, J. A.; Sung, K.; Jarvi, T. d.; Esswein, A. J.; Pijpers, J. J. H.; Nocera, D. G. *Science* **2011**, *334*, 645.
- (16) Duan, L.; Bozoglian, F.; Mandal, S.; Stewart, B.; Privalov, T.; Llobet, A.; Sun, L. *Nat. Chem.* **2012**, *4*, 418.
- (17) Duan, L.; Fischer, A.; Xu, Y.; Sun, L. *J. Am. Chem. Soc.* **2009**, *131*, 10397.
- (18) Xu, Y.; Åkermark, T.; Gyllai, V.; Zou, D.; Eriksson, L.; Duan, L.; Zhang, R.; Åkermark, B.; Sun, L. *Inorg. Chem.* **2009**, *48*, 2717.
- (19) Tong, L.; Duan, L.; Xu, Y.; Privalov, T.; Sun, L. *Angew. Chem., Int. Ed.* **2010**, *49*, 445.
- (20) Duan, L.; Xu, Y.; Gorlov, M.; Tong, L.; Andersson, S.; Sun, L. *Chem.—Eur. J.* **2010**, *16*, 4659.
- (21) Xu, Z.; Cotlet, M. *Angew. Chem., Int. Ed.* **2011**, *50*, 6079.
- (22) Lin, C.; Yeh, M.; Chen, C.; Sudhakar, S.; Luo, S.; Hsu, Y.; Huang, C.; Ho, K.; Luh, T. *Chem. Mater.* **2006**, *18*, 4157.
- (23) Yang, Y.; Rioux, R. M. *Chem. Commun.* **2011**, *47*, 6557.
- (24) Nakayama-Ratchford, N.; Bangsaruntip, S.; Sun, X.; Welsher, K.; Dai, H. *J. Am. Chem. Soc.* **2007**, *129*, 2448.
- (25) Chen, Z.; Concepcion, J. J.; Jurss, J. W.; Meyer, T. J. *J. Am. Chem. Soc.* **2009**, *131*, 15580.